Some Effects of the Shearing and Veering Environmental Wind on the Internal Dynamics and Structure of a Rotating Supercell Thunderstorm

Y. J. LIN AND P. T. CHANG

Department of Earth and Atmospheric Sciences, Saint Louis University, St. Louis 63103

(Manuscript received 16 January 1976, in revised form 4 May 1977)

ABSTRACT

A three-dimensional severe thunderstorm model is employed to study some effects that shearing and veering environmental winds exert on the structure and internal dynamics of a typical supercell rotating storm during its quasi-steady mature stage. These environmental winds are analytically formulated to conform with observations deduced from seven well-documented supercell storms. Horizontal relative winds are generated using the Rankine vortex concept for the inner core region (radii 0–4 km), the potential flow concept for the outer portion (radii 8–25 km) and the transition zone in between (radii 4–8 km). The temperature field is considered to conform with the observed warm-core structured storm. Using these semi-realistic data as input, six numerical experiments are conducted allowing the environmental wind to veer and to shear systematically from one case to another. Vertical velocities are obtained by solving the scaled mass continuity equation. Values of total pressure and perturbation pressure are computed from the diagnostic pressure equation obtained from the horizontal momentum equations using the sequential relaxation method. Results show that fields of perturbation pressure and vertical velocity are quite sensitive to the veering and shearing environmental wind in the region surrounding the central updraft core. Specifically, pronounced upward and downward motions are found on the right and left flank of a storm's updraft core, respectively. The magnitude of these induced vertical velocities increases in proportion to the vertical wind shear and is found to be closely related to perturbation pressure gradients. These findings are in good qualitative agreement with observational evidence reported in the literature. The role of these perturbation pressure forces in protecting the storm's main updraft is emphasized.

1. Introduction

Observational evidence has consistently revealed that the combined effects of potential instability and pronounced wind shears in the immediate environment of a severe thunderstorm are essential to its development and maintenance. Newton and Newton (1959) proposed a convective cloud model that included the generation of a vertical hydrodynamic pressure gradient in an area near the right flank of the cloud. Newton and Fankhauser (1964) postulated that deviation of the storm's movement to the right is primarily a result of new growth on the right flank of a storm, where low-level moisture is continually replenished together with the decay of convection on the left flank.

Recent studies of aircraft and Doppler wind measurements by Fujita and Grandoso (1968), Fankhauser (1971), Brown and Crawford (1972), Jessup (1972), Burgess (1974) Brown *et al.* (1975), etc., have shown that the updraft core region appears to force the environmental flow away from it. Based on seven years of aircraft measurements in Russia, Shmeter (1969) found that the middle and upper portions of storms are more likely to divert an environmental flow with a velocity maximum on the right and left flanks of the storm of up to 20–25 m s^{-1} stronger than the environmental wind. Such a flow field is somewhat analogous to potential fluid flow around a solid upright cylinder. The application of Doppler radar to the study of severe thunderstorms and their surroundings led Brown and Crawford (1972) to suggest that the storm's central updraft acts as an obstacle to the environmental flow. Their findings is consistent with the Doppler studies of Burgess (1974), Ray *et al.* (1975) and Kropfli and Miller (1976), and the chaff studies of Fankhauser (1971) and Jessup (1972), i.e., a severe thunderstorm is well-ventilated except for the core regions.

The main purpose of this study is to investigate some aspects of the role that shearing and veering environmental wind, relative to the movement of a typical rotating supercell storm, play in influencing the structure and internal dynamics of a storm during the mature stage of its life cycle. Only dynamic aspects of storm-environmental interactions in the middle and upper troposphere are stressed in the present study.

Fields of horizontal winds and temperature within a modeled storm and its immediate surroundings will be specified using derived formulas which are supported

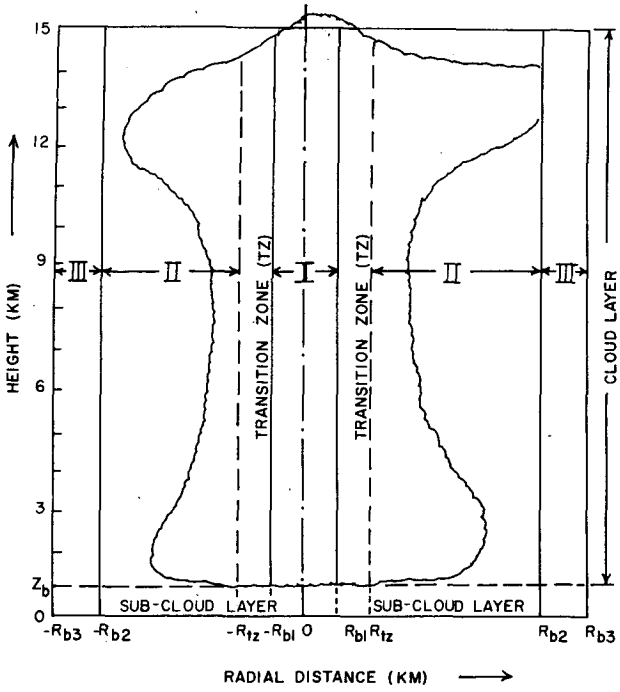

FIG. 1. A schematic diagram of the three-dimensional storm model during its quasi-steady mature stage. Values of R_{b1}, R_{tz}, R_{b2} and R_{b3} are assumed to be 4, 8, 25 and 30 km, respectively.

by a majority of recent observational studies of Doppler measurements and in-storm soundings. Values of pressure and temperature extracted from the tornado-proximity sounding of Darkow (1969) will be used as lateral boundary conditions for numerical integration. Using these specified values as input, the following quantities are then calculated throughout the domain of interest:

1. Fields of horizontal convergence (or divergence) from the horizontal wind components.
2. Vertical velocities from the mass continuity equation.
3. Fields of total pressure and perturbation pressure from the horizontal momentum equations.

Results obtained under each of six experiments are compared to available observed data whenever possible and are compared to the other experiments. Throughout these systematic comparisons, the relative importance of veering and shearing environmental air flow on structure and internal dynamics of a storm are emphasized.

2. The model

A three-dimensional rotating updraft severe thunderstorm model is devised to study important aspects of shearing and veering environmental wind effects on storm structure during the quasi-steady mature stage. The lowest layer ranges from the surface to a height of 1 km to represent the subcloud layer. The main body of the storm extends from the top of this layer (z_b) to a height $H = 15$ km (see Fig. 1). The horizontal extent of a model is assumed to be $R_{b3} = 30$ km from the storm's center. It is decomposed into four distinct regions, i.e., Regions I, II, III and the transition zone (TZ), to conform with a majority of observations for a typical supercell rotating storm. A detailed description of these four regions is given later.

In this study, the degree of shearing and veering environmental winds is allowed to vary to fit observational features summarized in Table 1. In this way, the relative importance of each of these effects on the structure and internal dynamics of a storm can be extracted from modeling responses by systematically comparing one case to another. For this reason, the magnitude of the environmental wind ($|\mathbf{V}_e|$) *relative to a traveling storm* with constant translational speed C is analytically specified as

$$|\mathbf{V}_e|(z) = V_{\max} \sin(\pi z/z_t). \tag{1}$$

Similarly, its veering with height is also analytically prescribed by the veering angle (β) with respect to westerly flow using the expression

$$\beta(z) = \beta_0 \exp[-B_1(z - z_b)]. \tag{2}$$

Thus, when $\beta(z) = 90°$, southerly flow predominates, while westerly wind is represented by $\beta(z) = 0°$. $V_{\max}$ and B_1 are two controlling parameters for determining the degree of shearing and veering, respectively. Z_t is assumed to be 20 km; β_0, the veering angle at cloud base (z_b), is considered to be 120°, and z_b is 1 km throughout the study.

In addition to the environmental relative wind vector ($\mathbf{V}_e$) described previously, this study requires consistent fields of horizontal winds and temperature within and around a storm as well as values of pressure, temperature and air density characteristic of the storm's environment for subsequent numerical experimentation. Since comprehensive data for any real storm do not exist, we generate these required data from certain well-known formulas using reliably observed values taken in the immediate environment of the storm as boundary conditions. The rationale behind such procedures has been extensively discussed in related studies of Lin and Martin (1971, 1972) and Lin and Hwang (1974).

On the basis of observational studies, the domain of a modeled storm is divided into the following four distinct regions:

a. Region I—inner core region

This region is chosen to range from the center of a modeled storm to radius R_{b1} of 4 km. It is intended to represent the updraft core region. Observational studies of Ray *et al.* (1975), Brown *et al.* (1975), Bonesteele

TABLE 1. A summary of certain gross features found in the environments of seven well-documented supercell storms.

Case study	Veering in subcloud layer (deg)	Mean wind surface to 10 km (deg/m s^{-1})	Storm motion (deg/m s^{-1})	Shear in cloud layer (10^{-3} s^{-1})
Browning and Donaldson (1963)	50	260/27	255/10	2.5
Browning (1965)	80	255/25	270/10	4.0
Haglund (1969)	60	265/25	280/14	2.5
Marwitz and Berry (1970)	90	250/17	285/14	4.5
Marwitz (1972)	60	250/15	320/9	4.0
Burgess (1974)	60	235/27	265/13	3.7
Bonesteele and Lin (1975)	50	260/15	290/13	3.6
Average	65	255/21.5	280/12	3.5

and Lin (1975), etc., and modeling studies of Lin and Martin (1972), Lin and Hwang (1974) lead us to suggest that relative horizontal wind fields within this core region for a typical supercell rotating storm can best be described by the combined Rankine vortex concept. Following this concept the east-west and north-south relative velocity components u_1 and v_1 are given by

$$u_1(x,y,z) = v_r x/r - v_\lambda y/r, \tag{3}$$

$$v_1(x,y,z) = v_r y/r + v_\lambda x/r, \tag{4}$$

where

$$v_\lambda = \left[\frac{2V_m r/r_m}{1+(r/r_m)^3}\right]\sin\left(\frac{\pi z}{H}\right), \tag{5}$$

$$v_r = \left[\frac{2U_n(z) r/r_m}{1+(r/r_m)^2}\right], \tag{6}$$

and r represents the radial distance from the storm's center. In the above v_λ and v_r denote tangential and radial velocity components, respectively; V_m (15 m s^{-1}) corresponds to the maximum value of v_λ and r_m (1.5 km) is the radius at which V_m occurs; and U_n is a height-dependent function which is assumed to be

$$U_n(z) = \begin{cases} -U_0^+ \cos\left(\dfrac{\pi z}{2z_c}\right), & z > z_c \\ -U_0^- \cos\left(\dfrac{\pi z}{2z_c}\right), & z \leqslant z_c \end{cases}$$

where z_c (6.8 km) is the height which separates the inflow layers from the outflow ones, $U_0^+ = 4.5$ m s^{-1} and $U_0^- = 2$ m s^{-1}. These expressions are shown to meet the mass continuity requirement (see Lin and Hwang, 1974).

b. Region II—potential flow region

The significance of this region in the outer portion of a storm and its immediate surroundings have been discussed by Shmeter (1969), Fankhauser (1971), Jessup (1972), Brown and Crawford (1972) and Kropfli and Miller (1976). It is assumed to extend from radii of R_{tz} (8 km) to R_{b2} (25 km) (see Fig. 1). Relative winds within this region, denoted by u_2 and v_2, can be generated from potential flow formulas

$$u_2 = -\frac{\partial \psi}{\partial y}, \quad v_2 = \frac{\partial \psi}{\partial x}.$$

Here the streamfunction $\psi(x,y,z)$ is given by

$$\psi(x,y,z) = -|\mathbf{V}_e|(z) y^* \left(1 - \frac{R_{bl}^2}{x^2+y^2}\right),$$

where

$$\left.\begin{aligned} y^* &= -x\sin\beta(z) + y\cos\beta(z) \\ R_{bl} &= (R_{b1}+R_{tz})/2 \end{aligned}\right\}.$$

c. Region TZ—transition zone between Regions I and II

This transitional region is assumed to cover from radii R_{b1} to R_{tz} throughout the domain of interest. It is designed to permit a transition between two distinct types of fluid flow regions, i.e., the Rankine-vortex-like flow in the inner core region of a storm (Region I) and the potential-flow-like circulation around the updraft core region in Region II. This design permits the interaction between Regions I and II in such a way that certain dynamic and kinematic boundary conditions are met. These include the continuity of pressure, temperature and wind components at $r = R_{b1}$ and $r = R_{tz}$. Relative winds in this region (u^* and v^*) are given by

$$u^*(x,y,z) = v_r^* x/r - v_\lambda^* y/r, \tag{7}$$

$$v^*(x,y,z) = v_r^* y/r + v_\lambda^* x/r, \tag{8}$$

where

$$v_r^* = (v_r)_{\text{at } R_{b1}} + [(v_r)_{\text{at } R_{tz}} - (v_r)_{\text{at } R_{b1}}][1-\cos(AG)],$$

$$v_\lambda^* = (v_\lambda)_{\text{at } R_{b1}} + [(v_\lambda)_{\text{at } R_{tz}} - (v_\lambda)_{\text{at } R_{b1}}][1-\cos(AG)],$$

$$AG = \frac{\pi(r-R_{b1})}{2(R_{tz}-R_{b1})}.$$

TABLE 2. Comparison between the observed and generated environmental wind shears in cloud layer for cases 1, 2 and 3.

Case	Shear	V_{max} (m s^{-1})	B_1 (km^{-1})	Average shears in cloud layer (10^{-3} s^{-1}) Observed	Generated
1	Weak	10	0.15	2.5	1.7
2	Moderate	20	0.15	3.5	3.4
3	Strong	30	0.15	4.5	5.0

d. Region III—storm's environment

This is the area at least 25 km away from the storm's center. It is characterized by an undisturbed environmental air flow under a clear sky as reported by many aircraft observations (e.g., Fujita and Grandoso, 1968; Fankhauser, 1971; Jessup, 1972; Sinclair, 1973; etc.). Relative winds u_3 and v_3 in this region are functions of height only so that

$$u_3(z) = |\mathbf{V}_e|(z)\cos\beta(z), \tag{9}$$

$$v_3(z) = |\mathbf{V}_e|(z)\sin\beta(z), \tag{10}$$

where $|\mathbf{V}_e|(z)$ and $\beta(z)$ are given in (1) and (2), respectively. The total wind vector $(\mathbf{V}_e)_t$ is readily obtained by adding the relative wind vector $\mathbf{V}_e$ to the storm translational vector $\mathbf{c}$, so that $(\mathbf{V}_e)_t = \mathbf{V}_e + \mathbf{c}$. Here $\mathbf{c}$ is considered constant throughout the storm depth with a direction and a speed of 280° and 12 m s^{-1}, respectively (see Table 1). V_{max} and B_1 in (1) and (2) are two important controlling parameters to specify the degree of shearing and veering for $\mathbf{V}_e$ in Region III. After comparing results of generated shears in cloud layers to those observed, we choose values of V_{max} to be 10, 20 and 30 m s^{-1} for representing a weak, moderate and strong shearing environment (see Table 2). B_1 values equal to 0.05, 0.15 and 0.30 km^{-1} denote an environmental wind with weak, moderate and strong veering (see Table 3). Figs. 2a and 2b illustrate generated environmental wind vector profiles for the six cases under investigation.

The generated relative winds $(\mathbf{V})_i$ at the 6 km level is shown in Fig. 3 for case 5. The subscript i indicates variables inside a storm. This field is calculated from (1) through (8) using $V_{max} = 20$ m s^{-1} and $B_1 = 0.15$ km^{-1}.

TABLE 3. Description of cases 4, 5 and 6 under investigation. Note that cases 2 and 5 are equivalent.

Case	Veer	V_{max} (m s^{-1})	B_1 (km^{-1})	Average shears in cloud layer (10^{-3} s^{-1}) Observed	Generated
4	Weak	20	0.05	3.5	3.4
5	Moderate	20	0.15	3.5	3.4
6	Strong	20	0.30	3.5	3.4

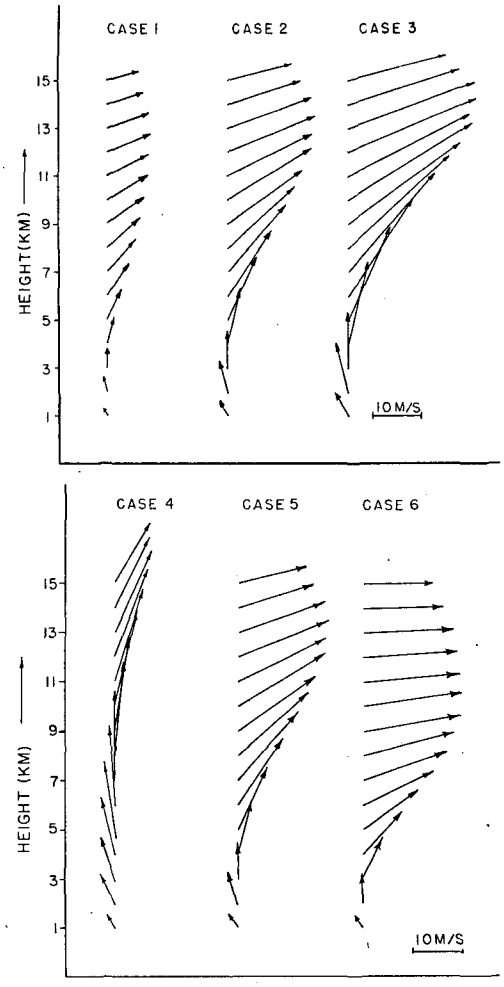

FIG. 2. Generated environmental wind vectors at various levels for cases 1, 2 and 3 (a) and cases 4, 5 and 6 (b).

In addition to relative winds discussed previously, the temperature field $T_i(x,y,z)$ is also considered as known using the tornado-proximity sounding of Darkow (1969) as a lateral boundary condition. It is given by

$$T_i(x,y,z) = \bar{T}(z) + T'(x,y,z).$$

Here $\bar{T}(z)$ is the environmental temperature deduced from Darkow's sounding and $T'(x,y,z)$ denotes the deviation from the mean. This quantity is analytically specified to conform with a warm-core structured storm so that

$$T'(x,y,z) = T_c\cos(\pi x/2X_b)\cos(\pi y/2Y_b)\sin(\pi z/H),$$

where T_c (6°C) is the maximum "excess" temperature occurring at the updraft core, X_b and Y_b are the outer boundary of Region II toward the x and y direction, respectively, and $X_b = Y_b = 25$ km.

The basic equations are the three momentum equations, the mass continuity equation, the thermodynamic energy equation and the equation of state. The mass continuity equation is scaled to become $\nabla_3\cdot[\bar{\rho}(z)\mathbf{V}]=0$,

where $\bar{\rho}(z)$ is environmental air density. The above form is consistent with that obtained by Ogura and Phillips (1962) for an anelastic system. The anelastic equations have been successfully employed by Wilhelmson (1974), Schlesinger (1975) and some others for numerical simulation studies of moist deep convection.

Since our main interest is to investigate interactions between a traveling storm and its immediate environmental wind field, it is convenient to employ a moving coordinate system (Fujita, 1963; Ninomiya, 1971; etc.). The momentum equations can be written as

$$u\frac{\partial u}{\partial x}+v\frac{\partial u}{\partial y}+w\frac{\partial u}{\partial z}=-\frac{1}{\rho}\frac{\partial p}{\partial x}+f(v+C_y), \tag{11}$$

$$u\frac{\partial v}{\partial x}+v\frac{\partial v}{\partial y}+w\frac{\partial v}{\partial z}=-\frac{1}{\rho}\frac{\partial p}{\partial y}-f(u+C_x), \tag{12}$$

$$u\frac{\partial w}{\partial x}+v\frac{\partial w}{\partial y}+w\frac{\partial w}{\partial z}=-\frac{1}{\rho}\frac{\partial p}{\partial z}-g, \tag{13}$$

where C_x and C_y are components of C toward the x and y axes, respectively, u, v and w are relative winds with respect to a traveling storm, and other symbols have their conventional physical meanings. Note that frictional terms are not considered in (11)–(13); they are assumed to be of secondary importance in comparison with other terms.

3. Procedures of numerical experiments

After obtaining the generated relative horizontal winds and temperatures, such quantities as vertical velocity (w), horizontal divergence ($\nabla_h\cdot\mathbf{V}_h$), total pressure ($P$) and perturbation pressure (P_d) can be calculated at grid points for each of the six cases described in Tables 2 and 3. Note that cases 2 and 5 are equivalent. The grid increment used for numerical integration is 0.5 km for all three directions. A centered differencing scheme was employed at all grid points except for the boundary points where a one-sided differencing scheme was used. Lateral boundary values of temperature ($\bar{T}$) and pressure ($\bar{P}$) were extracted from Darkow's tornado-proximity sounding and mean density ($\bar{\rho}$) was calculated from the equation of state.

a. Calculation of horizontal divergences and vertical velocities

Values of horizontal divergence in Region I and the transition zone (TZ) are readily obtainable from the specified wind field, i.e.,

$$\nabla_h\cdot\mathbf{V}_h=\frac{\partial u}{\partial x}+\frac{\partial v}{\partial y}. \tag{14}$$

In Region II where potential flow is dominant, $\nabla_h\cdot\mathbf{V}_h = 0$. The field of vertical velocity is calculated from the mass continuity equation

$$\frac{\partial[\bar{\rho}(z)w]}{\partial z}=-\bar{\rho}(z)\nabla_h\cdot\mathbf{V}_h \tag{15}$$

by integrating downward from the top of a modeled storm. Vertical velocities at the top (H = 15 km) are assumed to be zero.

b. Calculation of perturbation pressures

For the purpose of convenience, the total pressure field $P(x,y,z)$ is decomposed into two parts, *viz.*,

$$P(x,y,z) = \bar{P}(z) + P_d(x,y,z). \tag{16}$$

Here $\bar{P}(z)$ represents the environmental pressure and $P_d(x,y,z)$ the pressure departure from the mean environmental pressure $\bar{P}(z)$. It will be referred to as the "perturbation pressure" hereafter.

The P field is computed from the diagnostic pressure equation obtained from the horizontal momentum equations. Differentiating (11) with respect to x and (12) with respect to y, and adding yields

$$\nabla_h^2 p=\rho\left[\frac{\partial G(x,y,z)}{\partial x}+\frac{\partial H(x,y,z)}{\partial y}\right], \tag{17}$$

where

$$\nabla_h^2=\frac{\partial^2}{\partial x^2}+\frac{\partial^2}{\partial y^2},$$

$$G(x,y,z)=-u\frac{\partial u}{\partial x}-v\frac{\partial u}{\partial y}-w\frac{\partial u}{\partial z}+f(v+C_y)$$

$$H(x,y,z)=-u\frac{\partial v}{\partial x}-v\frac{\partial v}{\partial y}-w\frac{\partial v}{\partial z}-f(u+C_x).$$

Here the horizontal variation of air density is assumed to be small in comparison with other terms in (17) for pressure calculation. This assumption is justified by a scale analysis (not shown) using wind and temperature fields obtained.

Eq. (17) is solved by means of the sequential relaxation method using $\bar{P}(z)$ values as the lateral boundary condition. The overrelaxation coefficient used is 1.74.

4. Discussion of numerical results

This study has introduced certain idealizations to make the problem mathematically tractable. These include analytical specifications of relative wind fields and temperature values within the domain under investigation, and the assumption of quasi-steady conditions during the mature stage of a rotating supercell storm. Many of these idealizations have been justified, to a great extent, by factual evidence deduced from observation as discussed in previous sections. Since interactions between the storm and its veering

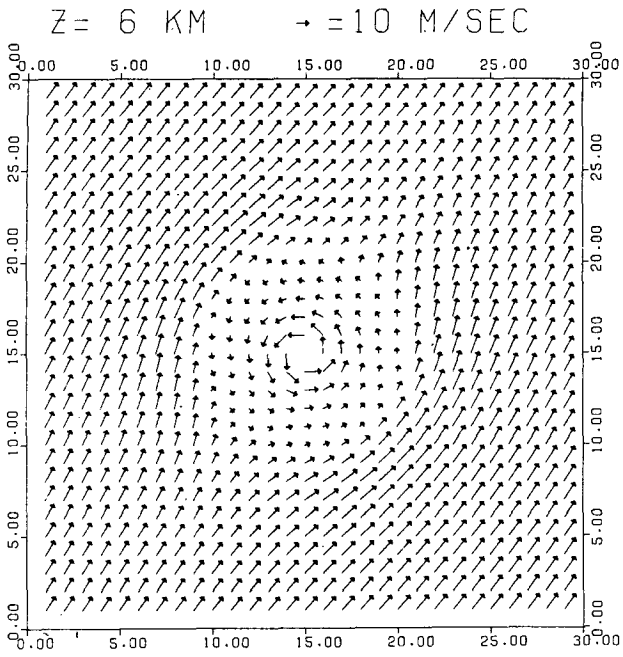

FIG. 3. Generated relative horizontal flow field at $z = 6$ km for case 5 (moderate shear and moderate veer). The domain covered is 30 km by 30 km on an x-y plane.

and shearing environmental wind are extremely complicated in nature, our findings are not expected to provide complete answers to these complex questions. Nevertheless, for the research to have value the derived quantities from the modeling equations must at least be in qualitative agreement with certain gross features of the mature storm. Various comparisons between the modeled storm and the real atmosphere will be presented whenever possible to show the similarities between the modeled responses and the observed results.

Six numerical experiments were conducted to investigate some effects that a shearing and veering environmental wind exerts on the structure and internal dynamics of a severe thunderstorm. Results under each experiment are so numerous, it is almost impossible to discuss them exclusively for all six cases being investigated. Instead, only results pertaining to case 5 will be discussed in great detail. For the other experiments, only those highlights of interest due to systematic comparisons of model responses from one case to another will be summarized. Note that since the above case is most consistent with the mean environment of a typical supercell storm found in the real atmosphere, our findings appear to have a considerable significance on the storm-environment interaction problem.

a. Vertical velocities

Spacial variation of vertical velocities (w) during the quasi-steady mature stage of a storm is of great importance in describing the internal dynamics and structure of that storm. Many observational studies, (e.g., Marwitz, 1973; Davies-Jones and Henderson, 1974; Ray *et al.*, 1975; Kropfli and Miller, 1976; etc.) have consistently revealed that severe storms consist of both downdrafts and updrafts. These drafts are characterized by a flow pattern which varies in all three spatial directions. Consequently, a three-dimensional treatment of flow fields is required to realistically represent circulation patterns within and around a storm.

Figs. 4–6 depict calculated w values at levels of 6, 9 and 12 km, respectively, for case 5. In these figures, $\bar{\mathbf{V}}_e$ denotes the vertically integrated relative environmental wind within a cloud layer, and $\mathbf{V}_e$ represents the relative environmental wind at any level under consideration. Since horizontal variations of w are found to be more significant within a 12 km radius of the storm's center, values of w external to this domain are not presented in these figures. It must be pointed out that a widely accepted concept of barrier flow (see Bates, 1961; Goldman, 1968; Fujita and Grandoso, 1968; Shmeter, 1969; Brown and Crawford, 1972; etc.) is shown to be most applicable to the middle and upper troposphere. In the lower troposphere, the problem of storm-environment interactions involves delicate interactions between the downdraft, primarily caused by the combined effects of precipitation drag and evaporation cooling, and the updraft, mainly induced by buoyancy and/or mechanical forces; for example, see the review papers of Ludlam (1963) and Newton (1963, 1967).

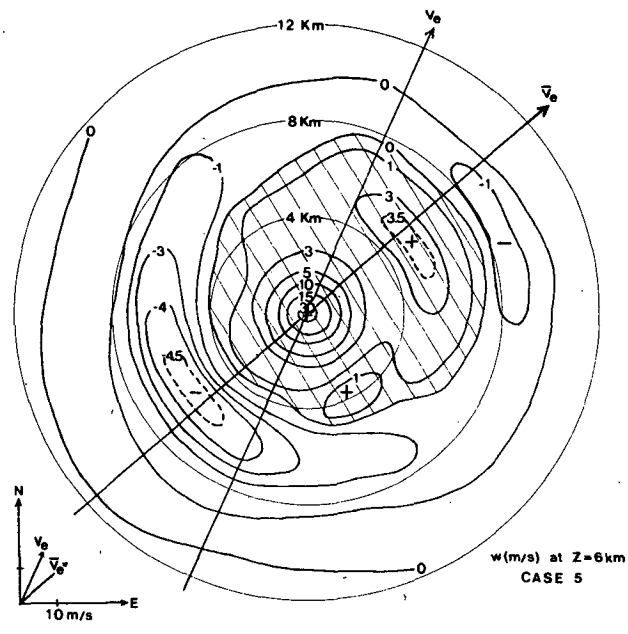

FIG. 4. Computed values of vertical velocity w (m s^{-1}) at $z = 6$ km for case 5 (moderate shear and moderate veer). The domain is covered by a 12 km radius from the storm's center. Shaded areas represent upward motions.

For this reason, discussions to follow will place primary emphasis on the middle and upper troposphere.

The calculated values of w together with the specified environmental relative wind vector ($\mathbf{V}_e$) at 6 km height are shown in Fig. 4. $\mathbf{V}_e$ at this level is coming from the southwest (214°). In the inner core region, a supercell with vertical speeds up to 30 m s^{-1} or greater dominates. The physical significance of this huge updraft on the structure and internal dynamics of a severe thunderstorm has been extensively studied by Lin and Martin (1972), Lin and Hwang (1974), Davies-Jones and Henderson (1974) and others. Around this core region, horizontal flow patterns become quasi-potential in character. As a result of storm-environment interactions, very pronounced upward motions (up to 4 m s^{-1}) are found on the right flank of a storm, while a slightly stronger downward motion ($\sim$5 m s^{-1}) prevails on the left flank. Interestingly enough, centers of these induced updrafts and downdrafts do rotate systematically, in a clockwise sense, with height in conjunction with the veering of an environmental relative wind ($\mathbf{V}_e$) (cf. Figs. 4–6). In other words, these "dynamically induced" updrafts and downdrafts around the central updraft core always occur on the right (forward) and left (rear) flanks of the storm's inner core, respectively.

In order to learn more as to how a shearing and veering environmental air flow affects the strength and location of such induced updrafts and downdrafts at any given height, additional numerical experiments described in Tables 2 and 3 were also conducted. Note that cases 1–3 only allow the magnitude of $\mathbf{V}_e$ to vary with height but the direction remains unchanged, whereas cases 4–6 only allow the direction of $\mathbf{V}_e$ to vary with height, while the magnitude remains the same. By systematically comparing one set of modelling responses to another for cases 4–6 (e.g., cf. Figs. 4, 7 and 8), we find that the effect of veering under a moderate shearing condition has a significant influence on the position of these induced drafts, but it does not have any effect on their strength.

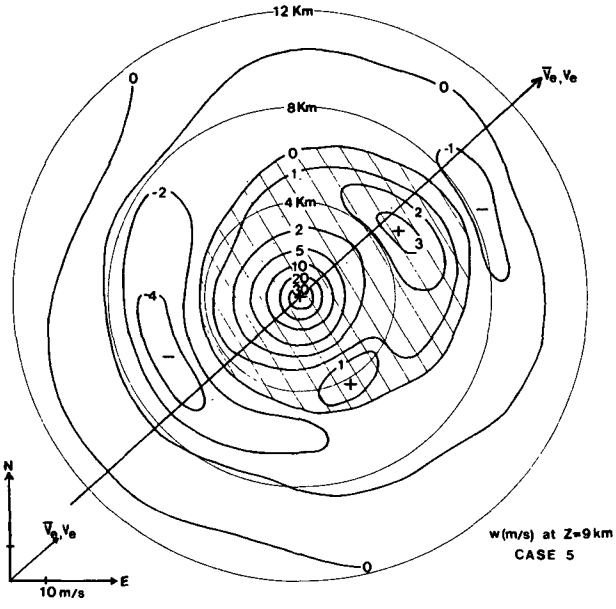

FIG. 5. As in Fig. 4 except for z = 9 km.

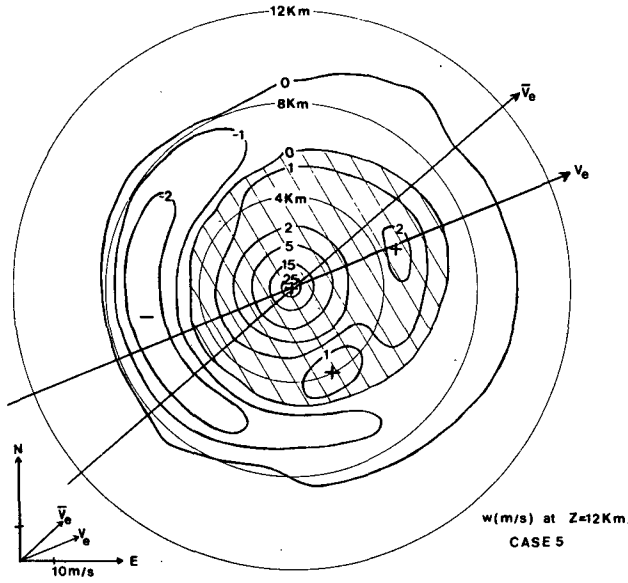

FIG. 6. As in Fig. 4 except for z = 12 km.

For cases 1–3, comparisons (not shown) indicate that the effect of wind shear $\partial|\mathbf{V}_e|/\partial z$ under a moderate veering condition has a significant bearing on the strength of these induced drafts, but it does not have any effect on their position. Thus, stronger shears of environmental wind tend to enhance upward displacements of air on the right flank of a storm and downward displacements on the left. Such enhanced upward motions on the right flank interact with any buoyancy forces already existing there and strengthen the release of latent heat by condensation. Newton and Fankhauser (1964) postulated that as a result of the new growth of cumulus clouds on the right flank, where low-level moisture is continuously transported upward to sustain deep moist convection, a cumulonimbus would deviate to the right of the vertically averaged mean environmental wind in the middle troposphere. On the other hand, enhanced downward motion on the opposite side (left flank) tends to suppress any existing buoyancy forces, thereby dissipating cumulus convection. The mid-level of this left flank, say, 500 mb or lower, is frequently cited as the most favorable spot for initiating a downdraft. The rationale behind this induced downdraft in relation to the processes of evaporative cooling and precipitation drag can be found in the studies of Bates (1961), Browning and Ludlam (1962), Newton (1966), Palmén and Newton (1969), Sinclair (1973) and Kropfli and Miller (1976).

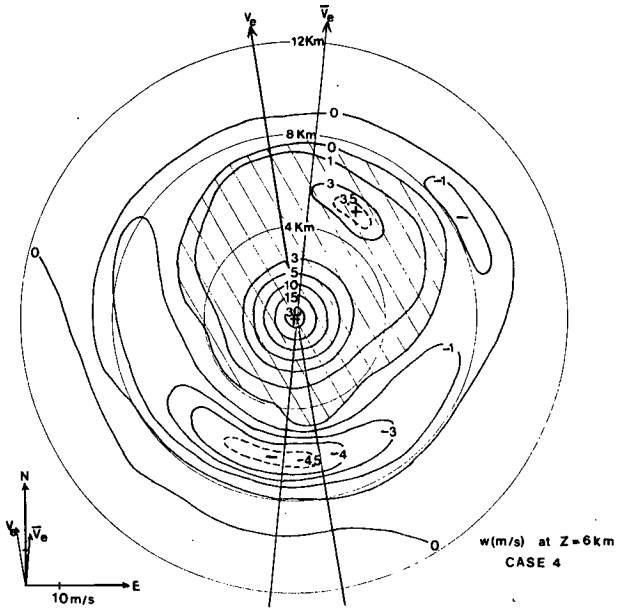

FIG. 7. As in Fig. 4 except for case 4 (moderate shear and weak veer) at $z = 6$ km.

On the basis of results obtained under experiments 1–6, we have shown that dynamical interactions, due to an on-rushing relative environmental air in the middle and upper troposphere interacting with a moving storm, tend to induce a unique field of vertical velocity around the inner updraft core (Region I) so that pronounced upward motions consistently occur on the right (forward) flank and downward motions prevail on the opposite side (left rear flank). The strength and position of these induced updrafts and downdrafts are solely determined by the directional shears $\partial \mathbf{V}_e/\partial z$, of a shearing and veering environmental wind ($\mathbf{V}_e$). Stronger shears would significantly increase the *intensity* of induced updrafts and downdrafts. The degree of veering, on the other hand, would determine the *position* of these draft centers with respect to the relative environmental wind vector $\mathbf{V}_e$ at a given height.

b. Perturbation pressures

The importance of pressure gradients in affecting intrinsic dynamics of cumulus convection and severe convective storms was studied by Van Thullenar (1960) and Fujita (1963). Using a simplified buoyancy equation only to include the terms of vertical acceleration and vertical "non-hydrostatic pressure," Fujita computed a field of "non-hydrostatic pressure" on a x-z plane of the well-known Browning and Ludlam (1962) kinematic model. He found that nonhydrostatic pressure gradients determine the vertical acceleration. A pressure difference of a few millibars separated by several kilometers height produces upward or downward motions on the order of 10 m s^{-1}. Similar results occur along the horizontal direction. Recent case studies of severe convective storms, e.g., Marwitz (1973), Davies-Jones and Henderson (1974), all stressed the findings of the so-called "cool updraft" in the layer near cloud base. Although temperature inside this cool updraft was reported to be 1–2°C cooler than its immediate surroundings, the updraft temperature became as much as 5–10°C warmer than its environment in the middle and upper layers. They attributed the main cause of this "nonbuoyant cool updraft" to the favorable vertical pressure gradient which is likely to force the relatively cool air upward into the lower portion of a storm's main updraft. Nevertheless, they cannot agree on the term "nonhydrostatic pressure" used. Since the basic pressures $\bar{P}(z)$ used to define the above term are those taken from environmental soundings rather than the local hydrostatic pressures, the term "perturbation pressure" should be used as suggested by Davies-Jones and Henderson (1974).

In this study, we have defined the perturbation pressure in the manner similar to that of Davies-Jones and Henderson (1974) [see Eq. (16)]. This quantity represents the combined effects of dynamic and thermodynamic processes taking place within and around a storm. These physical processes are not yet fully understood partly due to the lack of accurate pressure measurements within a storm. However, the perturbation pressure may well be deduced, within the range of acceptable accuracy, from modeling equations using the procedure suggested in Section 3 of this study.

Results of perturbation pressures (P_d) for case 5 on a horizontal plane, covered by a domain of 12 km radius, are shown in Figs. 9–11 for heights of 6, 9 and 12 km, respectively. It is seen that pressure excesses and deficits found around the core region (Region I) are

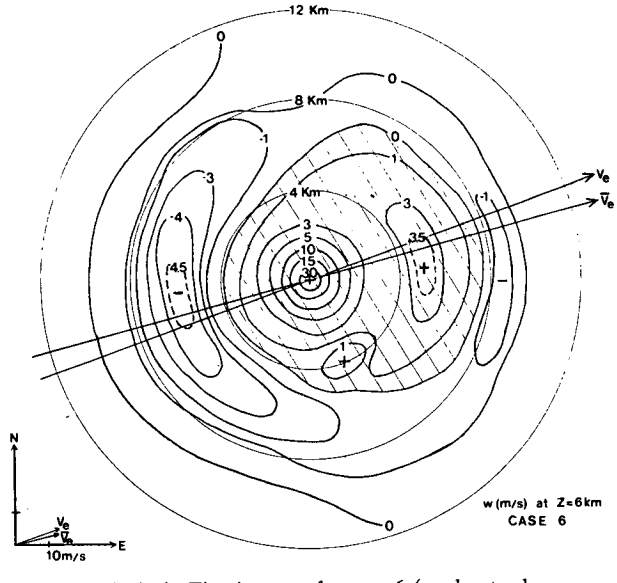

FIG. 8. As in Fig. 4 except for case 6 (moderate shear and strong veer) at $z = 6$ km.

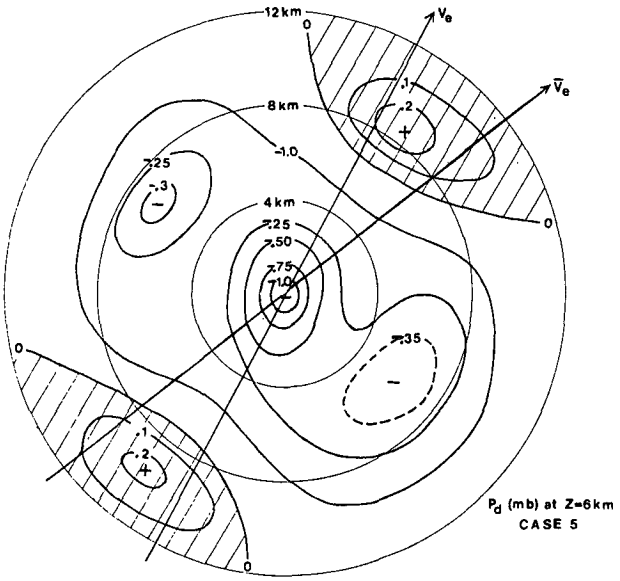

FIG. 9. Computed values of perturbation pressure P_d(mb) at $z = 6$ km for case 5 (moderate shear and moderate veer). The domain is covered by a 12 km radius from the storm's center. Shaded areas represent pressure excesses ($P_d > 0$).

attributed to storm-environment interactions. Such dynamical interactions tend to set up a P_d field with much smaller values on both right and left flanks, and larger values at the leading and trailing edge of a storm. Centers of the perturbation pressure around the central updraft are responsive to the environmental wind field. As shown in Figs. 9–11 they rotate clockwise with height in a manner similar to those of the w fields. Additional results obtained under other experiments (not shown) show further that horizontal and vertical

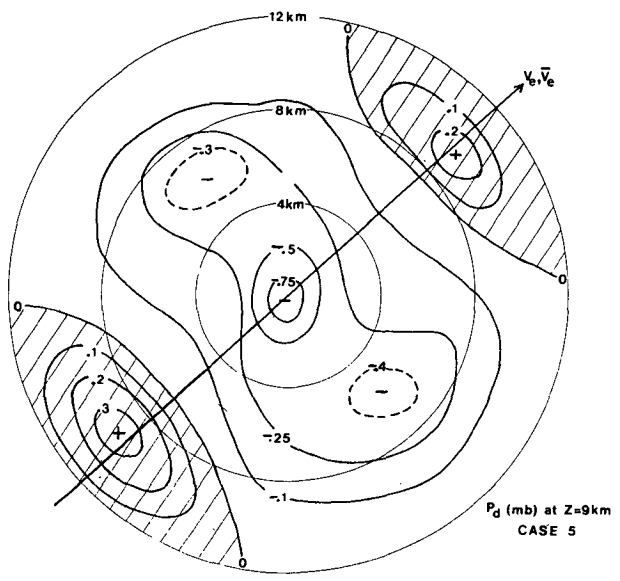

FIG. 10. As in Fig. 9 except for $z = 9$ km.

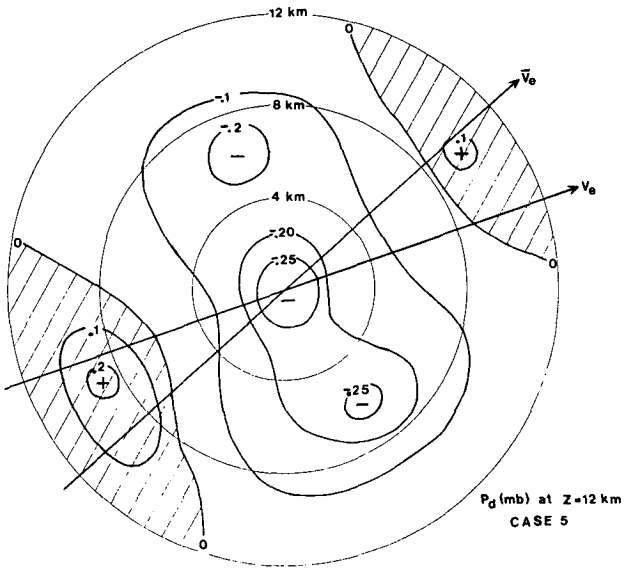

FIG. 11. As in Fig. 9 except for $z = 12$ km.

gradients of these perturbation pressures are intimately affected by environmental wind shears. Stronger (weaker) wind shears tend to provide stronger (weaker) perturbation pressure forces. As a result, very pronounced horizontal accelerations take place in the rear portion of right and left flanks, whereas a comparable magnitude of horizontal decelerations occurs on the front part of these two flanks. Furthermore, vertical P_d gradients are also pronounced over the "barrier flow layer" in particular. This feature is believed to be chiefly caused by dynamical interactions between an intruding environmental relative wind and the inner core of a storm. Many researchers [e.g., Newton (1963, 1967), Alberty (1969), etc.] suggest that such dynamically induced vertical P_d gradients are the most important mechanism in providing resistance to shearing forces exhibited by the environment of many severe convective storms. Our findings, however, tend to confirm that both horizontal and vertical P_d gradients around the storm's inner core are of vital importance in resisting shearing forces exerted on the updraft thereby prolonging the lifetime of a severe thunderstorm.

5. Summary and conclusion

A three-dimensional severe thunderstorm model is developed to study some effects of the veering and shearing environmental wind on the structure and internal dynamics of a typical rotating storm during its quasi-steady mature stage. Six numerical experiments with various veering and shearing conditions were conducted using semi-realistic data of horizontal winds and temperature as input. One set of results discussed in detail is that of the storm's environment

with a moderately veered and sheared relative wind. This type of an environmental air flow is observed to be most common over the Great Plains area. The results obtained are compared to available observed data reported in the literature. In addition, they are also systematically compared to those obtained under each of the other experiments being studied. Throughout such systematic comparisons the following conclusions are drawn:

1) Dynamical interactions between the storm's inner core and sheared and veered environmental winds tend to induce a vertical velocity field around the inner core region (Region I) in such a way that pronounced upward motions consistently occur on the right flank of the core and downward motions on the opposite side. Such enhanced upward motions on the right flank add to any buoyancy forces already existing there and tend to strengthen the new growth of convective cells over that region. Enhanced downward motions, on the other hand, would suppress any existing buoyancy forces on the left flank thereby contributing to the dissipation of cumulus convection on the left flank.

2) The intensity and position of these induced updrafts and downdrafts are closely related to the degree of shearing and veering of environmental air flow. Stronger shears significantly increase the intensity of these induced drafts. Their position is a function of the relative wind direction with height. Thus, a strongly sheared environmental wind can produce intense vertical motions around the inner core region so that the main updraft can be greatly protected from being entrained with drier environmental air.

3) Veered environmental winds produce a field of convergence and divergence, which is vertically nonaligned, around the storm's inner core region with convergence on the trailing edge of a storm's core and divergence on the opposite side.

4) Strong horizontal and vertical gradients of perturbation pressure are also induced around the inner core region as a result of storm-environment interactions. Pronounced pressure excesses are consistently found on the leading and trailing parts of a storm's core, whereas much larger magnitude of pressure deficits occurs on both flanks. The magnitude of these pressure gradient forces is *directly* proportional to environmental wind shears which in turn promote accelerations and decelerations of air motion around the main updraft core. As a result, air flow coming from the drier environment and outer portion of a storm is likely to be diverted away from the inner core region thereby minimizing the impact of lateral entrainment on the main updraft.

Our findings stated above are most applicable to those levels in the middle and upper troposphere where a slowly moving storm is totally exposed to an on-rushing environmental wind, and are in good qualitative agreement with those observed features deduced from well-documented supercell storms. Due to the lack of comprehensive observations for any single supercell storm to serve as standards of comparison, rigid statistical deductions of the results cannot be presented. Despite introducing several idealizations to make modeling efforts mathematically tractable, our results seem to capture certain relevant parameters as well as the role they play in the structure and internal dynamics of a storm. Nevertheless, we must realize that the effects discussed in this study may represent only a few aspects of an extremely complicated problem of storm-environment interactions. Persistence and maintenance of quasi-steady severe thunderstorm circulations during its mature stage are a combined result of dynamical and thermodynamical interactions throughout the whole domain of that storm. Furthermore, the movement of a storm is believed to be closely related to these dynamical and thermodynamical interactions. Certain remaining problems are under continuing investigation at Saint Louis University. These include: 1) To what extent is the movement of a supercell storm affected by storm-environment interactions? and 2) Why are such storms frequently found to deviate to the right (or occasionally to the left) of the mean environmental wind in the mid-troposphere?

Acknowledgments. We wish to thank Professor D. E. Martin and Dr. G. V. Rao of Saint Louis University for their many valuable suggestions and comments throughout this study. Appreciation is also extended to Captain R. Bonesteele of the U. S. Air Weather Service for his help in constructing the horizontal flow fields, and to Mrs. F. Brummell for typing the manuscript. This research has been supported by the Atmospheric Sciences Section, National Science Foundation, under Grant ATM74-09448 A02.

REFERENCES

Alberty, R. L., 1969: A proposed mechanism for cumulonimbus persistence in the presence of strong vertical shear. *Mon. Wea. Rev.*, **97**, 590–596.

Bates, F. C., 1961: The Great-Plains squall-line thunder-storm—a model. Ph.D. dissertation, St. Louis University, 164 pp.

Bonesteele, R., and Y. J. Lin, 1975: A numerical study of updraft-downdraft interactions during the mature stage of a rotating supercell thunderstorm using Doppler radar data. *Preprints 9th Conf. Severe Local Storms*, Norman, Okla., Amer. Meteor. Soc., 228–233.

Brown, R. A., D. W. Burgess, J. K. Carter, L. R. Lemon and D. Sirmaus, 1975: NSSL dual-Doppler radar measurements in tornadic storms: a preview. *Bull. Amer. Meteor. Soc.*, **56**, 524–526.

——, and K. C. Crawford, 1972: Doppler radar evidence of severe storm high-reflectivity cores acting as obstacles to air flow. *Preprints 15th Conf. Radar Meteorology*, Urbana, Ill., Amer. Meteor. Soc., 16–21.

Browning, K. A., 1965: A family outbreak of severe local storms—A comprehensive study of the storms in Oklahoma on 26 May 1963, Part I. Spec. Rep. No. 32, AFCRL-65-695(1), 346 pp.

——, and R. J. Donaldson, 1963: Airflow and structure of a tornadic storm. *J. Atmos. Sci.*, **20**, 535–545.

Browning, K. A., and F. H. Ludlam, 1962: Airflow in convective storms. *Quart. J. Roy. Meteor. Soc.*, **88**, 117–135.

Burgess, D. W., 1974: Study of a severe-right-moving thunderstorm utilizing new single Doppler radar evidence. M.S. thesis, Department of Meteorology, University of Oklahoma, 77 pp.

Darkow, G. L., 1969: An analysis of over sixty tornado proximity soundings. *Preprints 6th Conf. Severe Local Storms*, Chicago, Amer. Meteor. Soc., 182–183.

Davies-Jones, R. P., and J. H. Henderson, 1974: Updraft properties deduced from rawinsondings. NOAA Tech. Memo. GRL NSSL-72, 115 pp.

Fankhauser, J. C., 1971: Thunderstorm-environment interactions determined from aircraft and radar observations. *Mon. Wea. Rev.*, **99**, 171–192.

Fujita, T., 1963: Analytical mesometeorology: a review. *Meteor. Monogr.*, No. 27, Amer. Meteor. Soc., 77–125.

——, and H. Grandoso, 1968: Split of a thunderstorm into anticyclonic and cyclonic storms and motion as determined from numerical model experiments. *J. Atmos. Sci.*, **25**, 416–439.

Goldman, J. L., 1968: The high-speed updraft—The key to the severe thunderstorm. *J. Atmos. Sci.*, **25**, 224–248.

Haglund, G. T., 1969: A study of a severe local storm of 16 April 1967. NSSL Tech. Memo. No. 44, Norman, Okla., 54 pp.

Jessup, E. A., 1972: Interpretations of chaff trajectories near a severe thunderstorm. *Mon. Wea. Rev.*, **100**, 653–661.

Kropfli, R. A., and L. J. Miller, 1976: Kinematic structure and flux quantities in a convective storm from dual-Doppler radar observation. *J. Atmos. Sci.*, **33**, 520–536.

Lin, Y. J., and D. E. Martin, 1971: Some numerical aspects of a steady non-entraining severe storm with sloping updrafts. *J. Atmos. Sci.*, **28**, 1472–1478.

——, and ——, 1972: Further study of the severe storm with a rotating updraft configuration. *Tellus*, **24**, 216–228.

——, and H. J. Hwang, 1974: Some effects of the moisture distribution in the subcloud layer on the thermal structure of a mature severe thunderstorm. *Tellus*, **26**, 543–559.

Ludlam, F. H., 1963: Severe local storms: A review. *Meteor. Monogr.*, No. 27, Amer. Meteor. Soc., 1–32.

Marwitz, J. D., 1972: The structure and motion of severe hailstorms. Part I: supercell storms. *J. Appl. Meteor.*, **11**, 166–179.

——, 1973: Non-hydrostatic pressures in severe thunderstorms. *Preprints 8th Conf. Severe Local Storms*, Denver, Amer. Meteor. Soc., 14–17.

——, and E. X Berry, 1970: The weak echo region and updraft of a severe hailstorm. *Preprints 14th Conf. Radar Meteorology*, Tucson, Amer. Meteor. Soc., 43–47.

Newton, C. W., 1963: Dynamics of severe convective storms. *Meteor. Monogr.*, No. 27, Amer. Meteor. Soc., 33–58.

——, 1966: Circulations in large sheared cumulonimbus. *Tellus*, **18**, 699–713.

——, 1967: Severe convective storms. *Advances in Geophysics*, Vol. 12, Academic Press, 257–308.

——, and J. C. Fankhauser, 1964: On the movements of convective storms, with emphasis on size discrimination in relation to water-budget requirements. *J. Appl. Meteor.*, **3**, 651–668.

——, and H. R. Newton, 1959: Dynamical interaction between large convective cloud and environment wind vertical shear. *J. Meteor.*, **16**, 483–496.

Ninomiya, K., 1971: Dynamical analysis of outflow from tornado-producing thunderstorms as revealed by ATS III pictures. *J. Appl. Meteor.*, **10**, 275–294.

Ogura, Y., and N. A. Phillips, 1962: Scale analysis of deep and shallow convection in the atmosphere. *J. Atmos. Sci.*, **19** 173–179.

Palmén, E., and C. W. Newton, 1969: *Atmospheric Circulation Systems*. Academic Press, 405–414.

Ray, P. S., R. J. Doviak, G. B. Walker, D. Sirmans, J. Carter and B. Bumgarner, 1975: Dual-Doppler observation of a tornadic storm. *J. Appl. Meteor.*, **14**, 1521–1530.

Schlesinger, R. E., 1975: A three-dimensional numerical model of an isolated deep convective cloud: preliminary results. *J. Atmos. Sci.*, **32**, 934–957.

Shmeter, S. M., 1969: Structure of fields of meteorological elements in a cumulonimbus zone. [Israel Program for Scientific Translations, 1970, 117 pp.]

Sinclair, P. C., 1973: Severe storm air velocity and temperature structure deduced from penetrating aircraft. *Preprints 8th Conf. Severe Local Storms*, Denver, Amer. Meteor. Soc., 25–32.

Van Thullenar, C. F., 1960: Pressure difference between a cumulus cloud and its environment. *Proc. 1st Conf. Cumulus Convection*, Pergamon Press, 103–108.

Wilhelmson, R., 1974: The life cycle of a thunderstorm in three dimensions. *J. Atmos. Sci.*, **31**, 1629–1651.